PCCP

ROYAL SOCIETY OF CHEMISTRY

PAPER

View Article Online
View Journal | View Issue

Cite this: *Phys. Chem. Chem. Phys.*, 2024, **26**, 105

Water dynamics in eutectic solutions of sodium chloride and magnesium sulfate: implications for life in Europa's subsurface ocean and ice shell†

Daniel Sieme[c] and Nasrollah Rezaei-Ghaleh *[ab]

Received 20th July 2023,
Accepted 21st November 2023

DOI: 10.1039/d3cp03455k

rsc.li/pccp

Liquid water is essential for life as we know it and the coupling between water and biomolecular dynamics is crucial for life processes. Jupiter's moon Europa is a good candidate for searching for extraterrestrial life in our outer solar system, mainly because a liquid water salty ocean in contact with a rocky seafloor underlies its ice shell. Little, however, is known about the chemical composition of the subglacial ocean of Europa or the brine pockets within its ice shell and their impacts on water dynamics. Here, we employ ^{1}H, ^{17}O, ^{23}Na and ^{35}Cl NMR spectroscopy, especially NMR spin relaxation and diffusion methods, and investigate the mobility of water molecules and ions in eutectic solutions of magnesium sulfate and sodium chloride, two salts ubiquitously present on the surface of Europa, over a range of temperatures and pressures pertinent to Europa's subglacial ocean. The NMR data demonstrate the more pronounced effect of magnesium sulfate compared with sodium chloride on the mobility of water molecules. Even at its much lower eutectic temperature, the sodium chloride solution retains a relatively large level of water mobility. Our results highlight the higher potential of a sodium chloride-rich than magnesium sulfate-rich Europa's ocean to accommodate life and support life origination within the eutectic melts of Europa's ice shell.

Introduction

Jupiter's icy moon Europa is often regarded as a promising candidate for extraterrestrial life in the outer solar system. What makes Europa a particularly attractive candidate is that its >100 km deep subglacial liquid water ocean is in direct contact with a rocky seafloor, where geochemical processes such as hydrothermal activities could provide the sources of energy and nutrients required for a habitable environment.[1,2] Besides, the 3–30 km ice shell of Europa protects the subglacial ocean from the extremely cold temperature and UV irradiation of the surface, while at the same time, its unique plate tectonics and subduction[3] provides a route for the chemical exchange between the surface and subglacial ocean.[2] Consequently, oxidants produced photochemically or prebiotic molecules delivered by meteorites could be transported from the surface to the subsurface ocean.[4,5] The large dynamics of Europa's ocean, which are partly enhanced by its large aspect ratio of ~1/16,[6] could then promote the chemical exchange between the near-ice shell, bulk, and near-seafloor regions of the Europa's ocean and thereby bring together their complementary habitability advantages.

The habitability potential of Europa's subglacial ocean depends on various factors, including its salinity and chemical composition.[7] The salinity and chemical composition of Europa's ocean depends on the extent of water–rock interactions at the seafloor and transport of endogenous and exogenous materials from Europa's surface.[8–10] The estimated salinity varies depending on the assumed thickness of the ice shell, but the empirical data are consistent with very high salt concentrations similar to hypersaline lakes on Earth, if the ice shell of Europa is less than 15 km thick.[6,11] The dominant anionic type is suggested to be sulfate,[8,12–15] although, precipitation of gypsum ($CaSO_4 \cdot 2H_2O$) at the seafloor may reduce sulfate concentration and lead to a chloride:sulfate concentration ratio above 1 especially in near-ice regions.[10] An ocean composition with a high chloride concentration is consistent with recent spectroscopic observations suggesting the distinctive abundance of NaCl in the geologically young and disrupted chaotic regions of Europa's leading hemisphere.[16,17]

Cellular functions are mediated through biomolecular motions,[18] which are closely coupled to the dynamics of their

[a] *Heinrich Heine University (HHU) Düsseldorf, Faculty of Mathematics and Natural Sciences, Institute of Physical Biology, Universitätsstrasse 1, D-40225 Düsseldorf, Germany. E-mail: Nasrollah.Rezaie.Ghaleh@hhu.de*
[b] *Institute of Biological Information Processing, IBI-7: Structural Biochemistry, Forschungszentrum Jülich, Wilhelm-Johnen-Straße, D-52428 Jülich, Germany*
[c] *Department of NMR-based Structural Biology, Max Planck Institute for Multidisciplinary Sciences, Am Faßberg 11, D-37077 Göttingen, Germany*

† Electronic supplementary information (ESI) available: Supplementary methods and Fig. S1–S12. See DOI: https://doi.org/10.1039/d3cp03455k

surrounding water molecules.[19] The dissolved salts alter the structure and dynamics of water within the hydration shells of ions,[20,21] and a large body of empirical evidence suggests that the structural and dynamical impacts of dissolved salts may go beyond the hydration shells and influence the properties of bulk water.[22] The mutual dynamical coupling between ions, water and biomolecules is enhanced in the highly crowded and confined environments of the interior of cells and the subcellular compartments. Furthermore, considering that the current ''origin of life'' hypotheses frequently involve one or more environments of large confinement and/or high salt concentration, it is reasonable to assume that the coupling between ions and water dynamics could play a significant role in the generation and development of early life forms.[23]

On this background, the current study aims at characterizing water dynamics in aqueous salt solutions under compositions and laboratory conditions resembling those of the subsurface ocean of Europa. As for the salt, the current study is restricted to NaCl and $MgSO_4$, the two salts that according to our current best models are abundant in Europa's subsurface ocean. The eutectic concentrations of these two salts are utilized in order to minimize the freezing temperature of their solutions, hence extending the range of accessible temperatures downwards. More importantly, the eutectic solutions emulate the conditions of the eutectic melts potentially existing within the ice shell of Europa, where eutectic freezing can increase solute concentrations and promote the origin of life-related polymerization processes.[24] A range of temperature and pressure levels pertinent to Europa's subsurface ocean are explored. Under these conditions, we exploit NMR as the key technique and monitor the translational and rotational mobility of water molecules and ions through their nuclear spins, including quadrupolar spins ^{17}O, ^{23}Na and ^{35}Cl as well as the conventional ^{1}H spins. It is elucidated how water dynamics are affected by these two salts and its implications with regards to the habitability of Europa's subsurface ocean and its potential to support the origination of life are discussed.

Results

Properties of NaCl and $MgSO_4$ solutions

The mean salinity of Europa's ocean estimated from Galileo space probe's magnetometer-based ocean conductivities varies widely depending on the assumed thickness of the ice shell, but the empirical data are consistent with high salt concentrations if the ice shell would be less than 15 km thick.[11] Regardless of the mean global value for ocean salinity, a significant level of regional salinity variation is expected to occur near the rocky floor below or the icy shell above the ocean. Besides, the eutectic freezing within the icy shell of Europa may provide local environments with high salt concentrations close to eutectic concentrations.[24] Here, the NaCl and $MgSO_4$ solutions were prepared at eutectic concentrations, in which the freezing temperatures were reduced to −22.4 and −3.7 °C, respectively, hence allowing measurements at a broad range of temperatures. Obviously, these two salts are dissociated to their corresponding ions in aqueous solutions and lose their identity as salts. The molar concentration of eutectic NaCl and $MgSO_4$ solutions are about 3.953 and 1.446 M, respectively, implying an average cation–anion distance of 3.7 Å between Na^+ and Cl^- ions and 5.2 Å between Mg^{2+} and SO_4^{2-} ions. Considering that a water molecule has a diameter d_w of about 2.8 Å and Na^+, Cl^-, Mg^{2+} and SO_4^{2-} ions have water coordination numbers of respectively 6, 6, 6 and 7–12 in their first hydration shells,[20,22] a significant fraction of water molecules are expected to be placed inside the first hydration layer of the cation and/or anion, whereas less than *ca.* 15% of water molecules for the NaCl solution and 50–66% for the $MgSO_4$ solution act as the bulk water. Since water molecules exchange among the cationic and anionic hydration shells and bulk water at timescales faster than the so-called NMR chemical shift timescale, the measured NMR parameters of water dynamics will represent their population-weighted average in these (at least) three environments.

Rotational mobility of water in NaCl and $MgSO_4$ solutions

To monitor the rotational mobility of water (H_2O) molecules in NaCl and $MgSO_4$ solutions we studied NMR relaxation of their constituent proton (^{1}H) and natural abundance (^{17}O) nuclei, as discussed below.

^{1}H T_1 relaxation

The longitudinal spin–lattice (T_1) relaxation of water protons (^{1}H, spin I = 1/2) in aqueous salt solutions is predominantly governed by the intra- and inter-molecular proton–proton dipolar coupling, with the dipolar coupling between water proton and the NMR-active nuclei of the nearby ions providing additional minor contributions to ^{1}H T_1 relaxation. Since the strength of proton–proton dipolar coupling varies with the orientation of the inter-proton vector with respect to the external magnetic field as well as the inter-proton distance, the T_1 relaxation of water protons reflects both the rotational and translational dynamics of water molecules. The rotational correlation time (τ_c) of water molecules in pure water is around 1.5 ps at 298 K, indicating a motional regime for water molecules occurring on the left side of the T_1 minimum point. Consequently, an increase in τ_c *e.g.* through lowering temperature is expected to decrease the T_1 of water protons.

The 1D ^{1}H spectra of pure water and eutectic solutions of NaCl and $MgSO_4$ at a range of temperatures above their respective freezing temperatures are shown in Fig. 1(a) and Fig. S1a–c (ESI†). The T_1 relaxation of ^{1}H signals was then measured through saturation-recovery experiments, which are less prone to radiation-damping artefacts than inversion-recovery experiments.[25,26] The ^{1}H saturation-recovery data of pure water and eutectic NaCl and $MgSO_4$ solutions are demonstrated in Fig. 1(b) and Fig. S2a–c, ESI.† The obtained T_1 relaxation times in pure water and eutectic NaCl and $MgSO_4$ solutions are shown in Fig. 1(c). In pure water, the ^{1}H T_1 relaxation time exhibited a monotonic increase from 1.61 ± 0.01 s at 0 °C to 3.29 ± 0.01 s at 25 °C, reflecting the expected

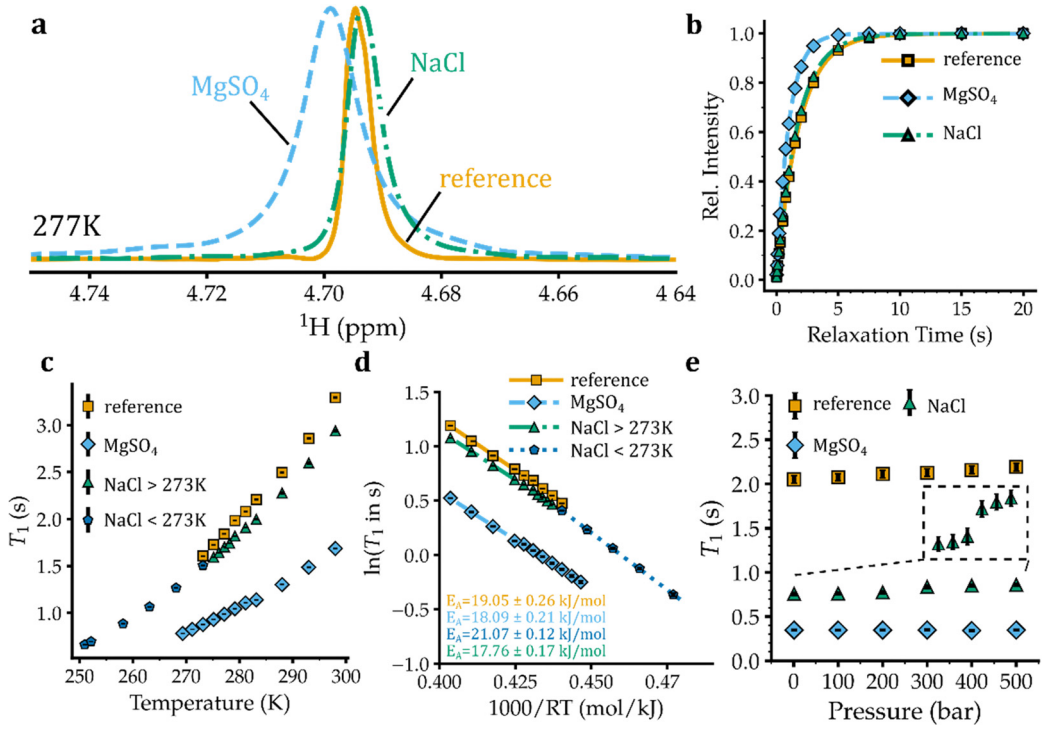

Fig. 1 Water mobility in reference (pure water) and eutectic NaCl and $MgSO_4$ solutions probed through ^1H longitudinal spin–lattice (T_1) relaxation times. (a), (b) 1D ^1H NMR spectra and saturation-recovery data of the mentioned samples shown as an example at 277 K (*ca.* 4 °C). (c) ^1H T_1 relaxation times, shown as a function of temperature from 298 K down to the freezing temperature of the mentioned samples. The T_1 relaxation time of water protons is smaller in NaCl and particularly $MgSO_4$ solutions than in the reference. (d) Arrhenius analysis of the temperature dependence of ^1H T_1 relaxation times. The slopes of the fitted lines represent the (apparent) activation energies (E_A) for ^1H relaxation-related water motions. (e) Pressure dependence of ^1H T_1 relaxation times, reported in the range 1–500 bar. Except for the NaCl solution (highlighted with a dashed area), no clear pressure dependence of ^1H T_1 is observed. The error bars shown in the different panels were derived from the standard error of the least-squares curve fitting and in some cases were smaller than the symbol size.

temperature-dependent enhancement of water mobility on the left side of the T_1 minimum. In eutectic NaCl solution, the T_1 relaxation time of water protons is slightly shorter than that of pure water and varied from 1.51 ± 0.01 s at 0 °C to 2.94 ± 0.02 s at 25 °C. However, the T_1 relaxation time of water protons in eutectic $MgSO_4$ solution is significantly shorter, ranging between 0.88 ± 0.01 and 1.69 ± 0.01 s at 0–25 °C. For both NaCl and $MgSO_4$ solutions the nearly linear temperature dependence of ^1H T_1 relaxation times extended down to temperatures near their freezing temperatures of −22.4 and −3.7 °C, respectively (Fig. 1(c)). Notably, at the eutectic temperatures of *ca.* −22.2 and −3.7 °C for the NaCl and $MgSO_4$ solutions, the ^1H T_1 relaxation times of water were 0.66 ± 0.01 and 0.78 ± 0.01 s, respectively. The Arrhenius analysis of temperature dependence of ^1H T_1 relaxation times yielded (apparent) activation energies (E_A) of 19.05 ± 0.26 kJ mol^{-1} for pure water and 17.76 ± 0.17 kJ mol^{-1} for eutectic $MgSO_4$ solution, representing the energy barrier against rotational and coupled translational motion of water molecules. In the case of the eutectic NaCl solution, the E_A obtained at a similar temperature range (0–25 °C) was 18.09 ± 0.21 kJ mol^{-1}, while at temperatures lower than 0 °C a slightly larger E_A of 21.07 ± 0.12 kJ mol^{-1} was obtained (Fig. 1(d)). Overall, the ^1H T_1 data indicated that, despite its smaller concentration and larger fraction of water molecules outside the first coordination layer of ions, the eutectic $MgSO_4$ solution exhibited lower water mobility than the eutectic NaCl solution. The lower water mobility in $MgSO_4$ solution is therefore related to ion types and their characteristics such as electric charges, not ion concentration. At their corresponding eutectic temperatures, however, the water mobility was slightly higher in the $MgSO_4$ than in the NaCl solution.

Next, we investigated the pressure dependence of ^1H T_1 relaxation times of water in the eutectic solutions of NaCl and $MgSO_4$. Because the gravitational acceleration of Europa is less than one seventh that of the Earth, the hydrostatic pressures in the Europa's ocean are proportionally smaller than Earth oceans at the same depth levels.[24] For example, the pressure level at 4 km depth of Earth oceans, where many large and complex forms of life are found,[27] is 40 MPa (400 bar), comparable to the pressure level of the Europa's ocean at *ca.* 30 km depth. Accordingly, we measured ^1H NMR experiments at pressure levels of 0.1–50 MPa (1–500 bar), corresponding to depth levels up to *ca.* 38 km in Europa's ocean. The pressure increase to 50 MPa is expected to reduce the eutectic temperature of NaCl and $MgSO_4$ solutions even further by *ca.* 4 °C, as shown recently.[28] However, due to limitations of the high-pressure ceramic NMR tube, the measurements were

performed at 5 °C, the lowest allowed temperature for that kind of NMR tube. The obtained 1D ^{1}H spectra of pure water and eutectic solutions of NaCl and $MgSO_4$ are shown in the ESI,† Fig. S3a–c. The ^{1}H saturation-recovery data of corresponding samples provided ^{1}H T_1 relaxation times (Fig. S4a–c, ESI† and Fig. 1(e)): in pure water, the ^{1}H T_1 showed little pressure dependence varying from 2.05 ± 0.04 s at ambient pressure to 2.19 ± 0.04 s at 500 bar. Unlike pure water, the eutectic NaCl solution exhibited some pressure-dependent ^{1}H T_1 variation especially evident between 200 and 300 bar (Fig. 1(e)). The ^{1}H T_1 of water in the eutectic NaCl solution varied between 0.76 ± 0.02 and 0.86 ± 0.02 s over the pressure range of 1–500 bar. Similar to pure water, the eutectic $MgSO_4$ solutions did not show a significant pressure dependence of ^{1}H T_1 relaxation times (Fig. 1(e)). Considering that around 85% of water molecules in NaCl solution (*versus* 34–50% in $MgSO_4$) are located in ion hydration layers, we speculate that the small pressure-dependence of ^{1}H T_1 in NaCl solution is caused by a pressure-dependent change in the hydration sphere of sodium and/or chloride ions. At all the studied pressure levels, the ^{1}H T_1 followed the order of pure water > eutectic NaCl > eutectic $MgSO_4$, indicating the same order of water mobility in these solutions. It is expected that the order of ^{1}H T_1, hence of water mobility, does not change when pressure is increased up to 800–2000 bar, corresponding roughly to the depth levels of 60–150 km in Europa's ocean.

^{17}O T_1 relaxation

Around 0.037% of water molecules contain the rare oxygen isotope of ^{17}O. The ^{17}O nucleus has a quantum spin number I of 5/2 and $2I + 1 = 6$ energy levels (represented as $|-5/2\rangle$, $|-3/2\rangle$, $|-1/2\rangle$, $|+1/2\rangle$, $|+3/2\rangle$, $|+5/2\rangle$). The NMR signal of ^{17}O therefore consists of one central transition (CT: $|-1/2\rangle \leftrightarrow |+1/2\rangle$) and two pairs of satellite transitions (ST: $|\pm1/2\rangle \leftrightarrow |\pm3/2\rangle$ and $|\pm3/2\rangle \leftrightarrow |\pm5/2\rangle$). Due to the fairly large quadrupole moment Q of ^{17}O, the T_1 relaxation of ^{17}O is almost entirely governed by the highly efficient anisotropic interaction between its electric quadrupole moment (eQ) and the electric field gradient (EFG) tensor present at the site of each ^{17}O nuclei. In the fast extreme-narrowing regime of motion where $\omega_0\tau_c \gg 1$ (ω_0, Larmor frequency, τ_c, rotational correlation time), the one CT and two ST components of the ^{17}O signal share the same T_1 relaxation times, which is inversely proportional to τ_c, hence reports the rotational dynamics of water molecules.[29]

The 1D natural abundance ^{17}O spectra of pure water and eutectic solutions of NaCl and $MgSO_4$ are shown in Fig. 2(a) and Fig. S5a–c, S6, ESI.† As expected, in the $MgSO_4$ solution, the ^{17}O nuclei of sulfate ions had a chemical shift of *ca.* 167 ppm (Fig. S6, ESI†), which is far from the ^{17}O NMR signal of water molecules shown in Fig. 2(a). The T_1 relaxation of ^{17}O signals was then measured through standard inversion–recovery experiments, in which the ^{17}O signals exhibited single-exponential intensity recovery curves (Fig. 2(b) and Fig. S7a–c, ESI†). In pure water, the obtained ^{17}O T_1 relaxation times ranged from 4.09 ± 0.08 ms at 5 °C to 7.29 ± 0.13 ms at 25 °C (Fig. 2(c)), in close agreement with previous reports.[30] The eutectic NaCl solution showed significantly shorter ^{17}O T_1 relaxation times ranging from 3.05 ± 0.05 at 5 °C to 5.57 ± 0.10 ms at 25 °C (Fig. 2(c)). In the eutectic $MgSO_4$ solution, the ^{17}O T_1 relaxation times were considerably shorter than those of pure water and even the NaCl solution: they ranged from 1.61 ± 0.17 at 5 °C to 3.66 ± 0.06 ms at 25 °C (Fig. 2(c)). The Arrhenius analysis of temperature dependence of ^{17}O T_1 relaxation times yielded (apparent) E_A of 19.78 ± 1.03 kJ mol^{-1} for pure water and 20.03 ± 1.11 kJ mol^{-1} for eutectic NaCl (Fig. 2(d)). For the eutectic $MgSO_4$ solution, a non-linear Arrhenius curve was observed: the estimated E_A was 18.61 ± 0.33 kJ mol^{-1} at 288–298 K, similar to the values obtained for pure water and the eutectic NaCl solution. However, at lower temperatures of 278–288 K, the estimated E_A exhibited a two-fold increase to 38.62 ± 1.03 kJ mol^{-1}. While the obtained ^{1}H and ^{17}O T_1-based E_A of water molecules in pure water were within the experimental range of error identical with each other, the ^{17}O T_1-based (apparent) E_A of water molecules in the eutectic NaCl and particularly $MgSO_4$ solution at lower temperatures were larger than the ^{1}H T_1-based ones. The observed discrepancies suggest that, in the NaCl and particularly $MgSO_4$ solution, the temperature-dependent changes in the structure of water (averaged between bulk water and water in hydration layers) and the resultant alterations of the EFG tensor at the site of water's ^{17}O nuclei make a significant contribution to temperature dependence of ^{17}O T_1 relaxation times. On the other hand, this effect is much smaller in pure water, suggesting that the effect observed in NaCl and $MgSO_4$ solutions predominantly originated from structural alterations of water in hydration layers. Overall, the ^{17}O T_1 data were consistent with the lower rotational mobility of water molecules in the eutectic $MgSO_4$ compared with the NaCl solution, as indicated by ^{1}H T_1 data (see above).

Translational mobility of water in NaCl and $MgSO_4$ solutions

Next, we studied the diffusion of water molecules through pulse-field-gradient NMR (PFG-NMR) diffusion experiments. In this method, the magnetic field gradients applied along the z-axis enables spatial labeling of the studied nuclei and allows probing their translational mobility along the same axis.[31] The diffusion of water molecules was monitored through their ^{1}H NMR signals, as the relaxation of their natural abundance ^{17}O signal was too fast to survive the relatively long diffusion delay. The ^{1}H-based diffusion coefficients of water molecules in pure water and eutectic NaCl and $MgSO_4$ solutions at a range of temperature are shown in Fig. 3(a) and (b) and Fig. S8a–c, ESI.† In pure water, the diffusion coefficient of water rose from 1.042 ± 0.002 × 10^{-9} m^2 s^{-1} at 0 °C to 2.286 ± 0.024 × 10^{-9} m^2 s^{-1} at 25 °C. The diffusion coefficient of water in NaCl and particularly $MgSO_4$ solutions were significantly smaller than that of pure water within the same temperature range. All three samples exhibited nearly linear temperature dependences down to their freezing temperatures. At the corresponding eutectic temperatures of *ca.* −22.2 and −3.7 °C for the NaCl and $MgSO_4$ solutions, the diffusion coefficients of water were 0.328 ± 0.013 × 10^{-9} m^2 s^{-1} and

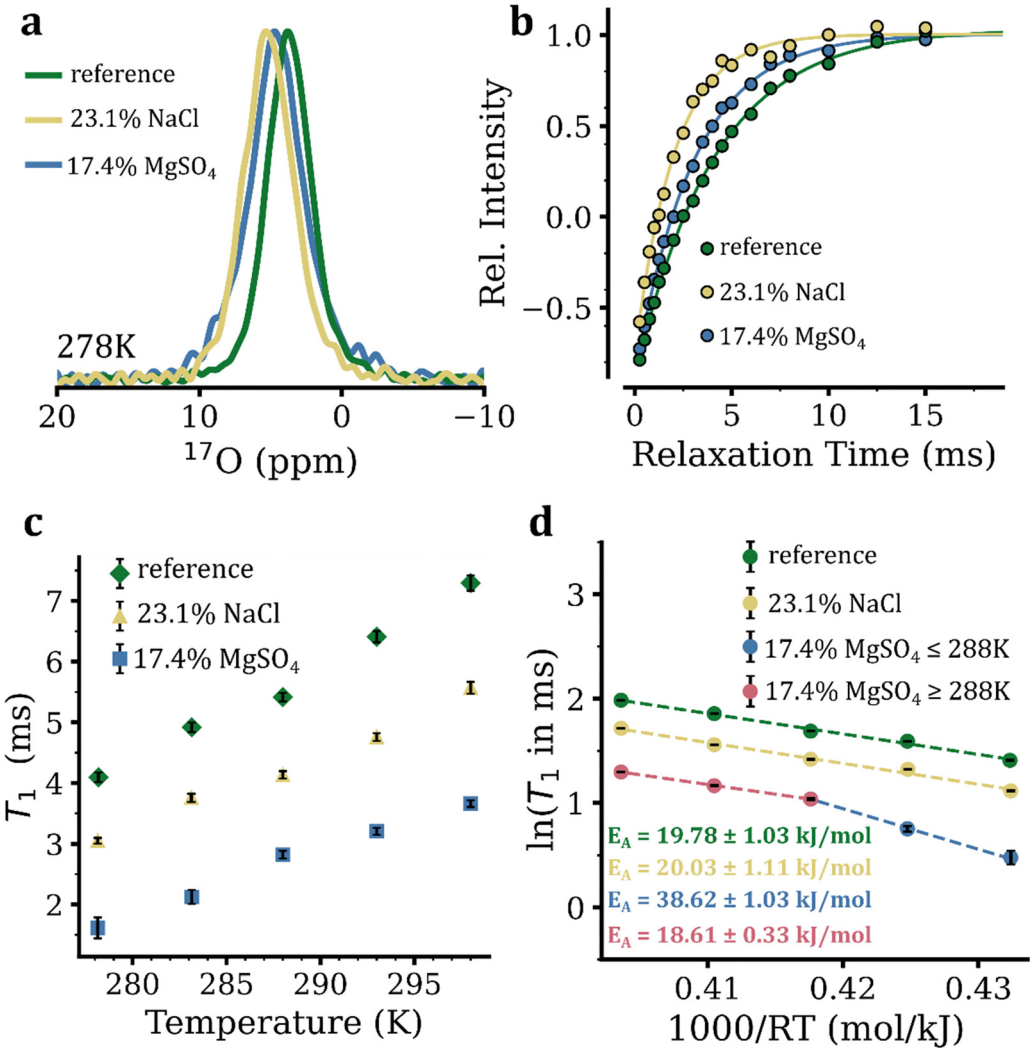

Fig. 2 Water mobility in reference (pure water) and eutectic NaCl and $MgSO_4$ solutions probed through ^{17}O longitudinal spin–lattice (T_1) relaxation times. (a), (b) 1D ^{17}O NMR spectra and inversion-recovery data of the mentioned samples shown as an example for the temperature of 5 °C. (c) ^{17}O T_1 relaxation times, shown as a function of temperature in the range 278–298 K. The ^{17}O T_1 relaxation times of water is the smallest in $MgSO_4$ solution, followed by the NaCl solution. (d) Arrhenius analysis of the temperature dependence of ^{17}O T_1 relaxation times. The slopes of the fitted lines represent the (apparent) activation energies (E_A) for the rotational mobility of water molecules. The error bars shown in the different panels were derived from the standard error of the least-squares curve fitting and in some cases were smaller than the symbol size.

$0.461 \pm 0.015 \times 10^{-9}$ m^2 s^{-1}, respectively. Based on the Arrhenius analysis of temperature dependence of diffusion coefficients, the (apparent) E_A of 21.47 ± 0.26 kJ mol^{-1} for pure water and 21.55 ± 0.14 kJ mol^{-1} for eutectic $MgSO_4$ solution was obtained (Fig. 3(c)). In the case of the eutectic NaCl solution, the E_A obtained at a similar temperature range (0–25 °C) was 19.77 ± 0.12 kJ mol^{-1}, while at temperatures lower than 0 °C a larger E_A of 22.61 ± 0.22 kJ mol^{-1} was obtained (Fig. 3(c)). In general, the obtained diffusion-based E_A were slightly larger than the ^1H (and in case of pure water and eutectic NaCl solutions, also ^{17}O) T_1-based E_A (see above). Overall, the diffusion data indicated a lower translational mobility of water molecules in the eutectic $MgSO_4$ than in NaCl solution. At their corresponding eutectic temperatures, however, the translational mobility of water was slightly higher in the $MgSO_4$ than in the NaCl solution.

Subsequently, the diffusion coefficients of water in pure water and eutectic salt solutions were measured at 5 °C and pressure levels of 1–500 bar. In pure water, the diffusion coefficient of water slightly increased with pressure, while that of water in eutectic salt solutions did not show any significant pressure dependence (Fig. 3(d) and Fig. S9a–c, ESI†). At all the studied pressure levels, the same order of water's translational mobility, that is pure water > eutectic NaCl solution > eutectic $MgSO_4$ solution, was observed. The order of water's translational mobility is expected to remain the same up to 2000 bar, the pressure level corresponding to a depth level of *ca.* 150 km in Europa's ocean.

Rotational and translational mobility of ions in NaCl solution

Recent NMR-based studies have shown a high level of independent mobility of ions within saturated salt solutions and

phase-separated highly confined environments of biological hydrogels.[30,32,33] To monitor the mobility of sodium and chloride ions inside the eutectic NaCl solution, we utilized the ^{23}Na- and ^{35}Cl-based NMR as detailed below. Similar experiments for the eutectic $MgSO_4$ solution were possible only for the ^{17}O nuclei of sulfate ions, as the naturally abundant isotopes of sulfur in sulfate anion are NMR silent or intractable and the low-γ ^{25}Mg nucleus has a Larmor frequency well below the lower frequency limit of the NMR probe used in this study.

^{23}Na and ^{35}Cl T_1 relaxation of ions in eutectic NaCl solution

The ^{23}Na and ^{35}Cl isotopes represent almost 100% and 75.76% of sodium and chloride ions in nature. The ^{23}Na and ^{35}Cl nuclei have a quantum spin number I of 3/2 and $2I + 1 = 4$ energy levels (represented as $|-3/2\rangle$, $|-1/2\rangle$, $|+1/2\rangle$, $|+3/2\rangle$). Consequently, the NMR signals of these nuclei consist of one central transition ($|-1/2\rangle \leftrightarrow |+1/2\rangle$) and one pair of satellite transitions ($|\pm1/2\rangle \leftrightarrow |\pm3/2\rangle$). Similar to ^{17}O, the quadrupolar relaxation mechanism is the main mechanism underlying the T_1 relaxation of these two nuclei. With sodium and chloride ions moving in the fast extreme-narrowing regime, as defined above, the T_1 relaxation time of ^{23}Na and ^{35}Cl nuclei becomes inversely proportional to τ_c hence reflects the rotational mobility of sodium and chloride ions.[34,35]

The 1D ^{23}Na and ^{35}Cl NMR spectra of the eutectic NaCl solution at temperatures 5–25 °C are shown in Fig. 4(a) and 5(a). The inversion-recovery data supported the mobility of sodium and chloride ions occurring within the fast extreme-narrowing regime, as the NMR signal intensity recovery of these quadrupolar nuclei obeyed an apparent single-exponential curve (Fig. 4(b) and 5(b)). As expected for their shorter rotational correlation time at higher temperatures (see the ESI,† eqn (S3)), the T_1 relaxation times of ^{23}Na and ^{35}Cl nuclei exhibited a monotonic temperature-dependent increase between 5 and 25 °C (Fig. 4(c) and 5(c)). The ^{23}Na T_1 relaxation times rose from 28.872 ± 0.002 ms at 5 °C to 43.444 ± 0.003 ms at 25 °C. Notably, the ^{23}Na T_2 relaxation times estimated from the linewidths (T_2*) of ^{23}Na signals were almost identical to the T_1 relaxation times: T_2* were 27.6 and 41.2 ms respectively at 5 and 25 °C. This further supports the dynamics of sodium ions

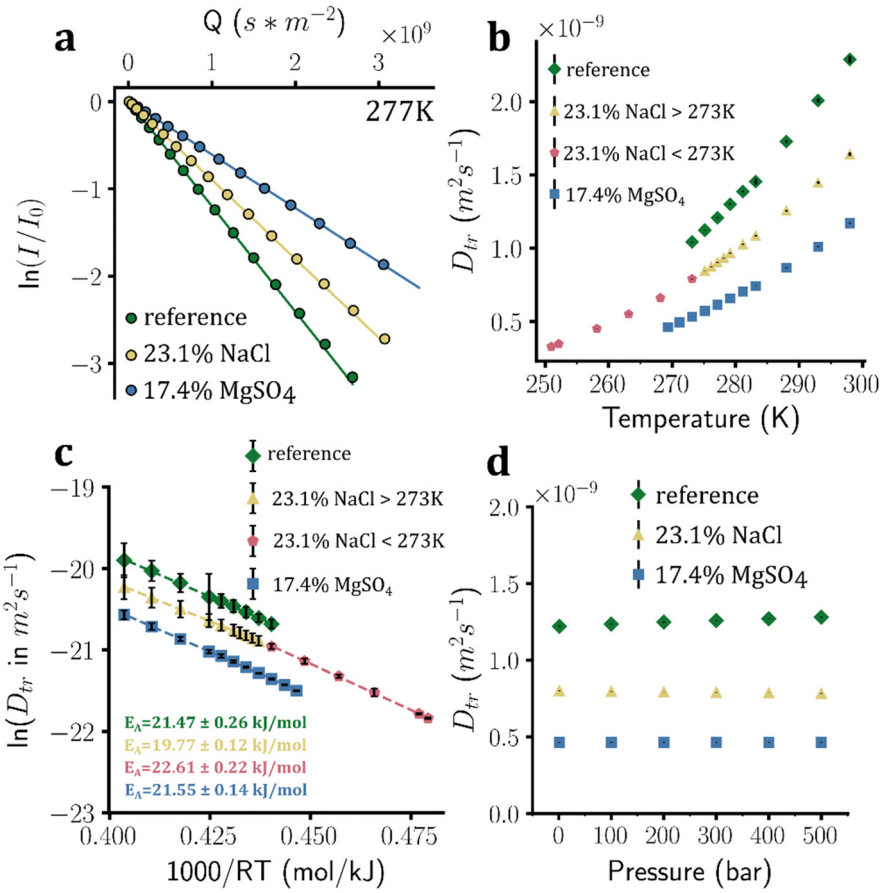

Fig. 3 Water diffusion in reference (pure water) and eutectic NaCl and $MgSO_4$ solutions probed through ^{1}H pulse-field-gradient (PFG) NMR diffusion experiments. (a) Gradient-dependent intensity attenuation data of the mentioned samples in PFG-NMR experiments, shown as an example for the temperature of 4 °C. (b) Diffusion coefficient of water, shown as a function of temperature from 298 K down to the freezing temperature of the mentioned samples. (d) Arrhenius analysis of the temperature dependence of water diffusion coefficients. The slopes of the fitted lines represent the (apparent) activation energies (E_A) for translational diffusion of water molecules. (d) Diffusion coefficients of water as a function of pressure at 278 K. No clear pressure dependence was observed. The error bars shown in the different panels were derived from the standard error of the least-squares curve fitting and in some cases were smaller than the symbol size.

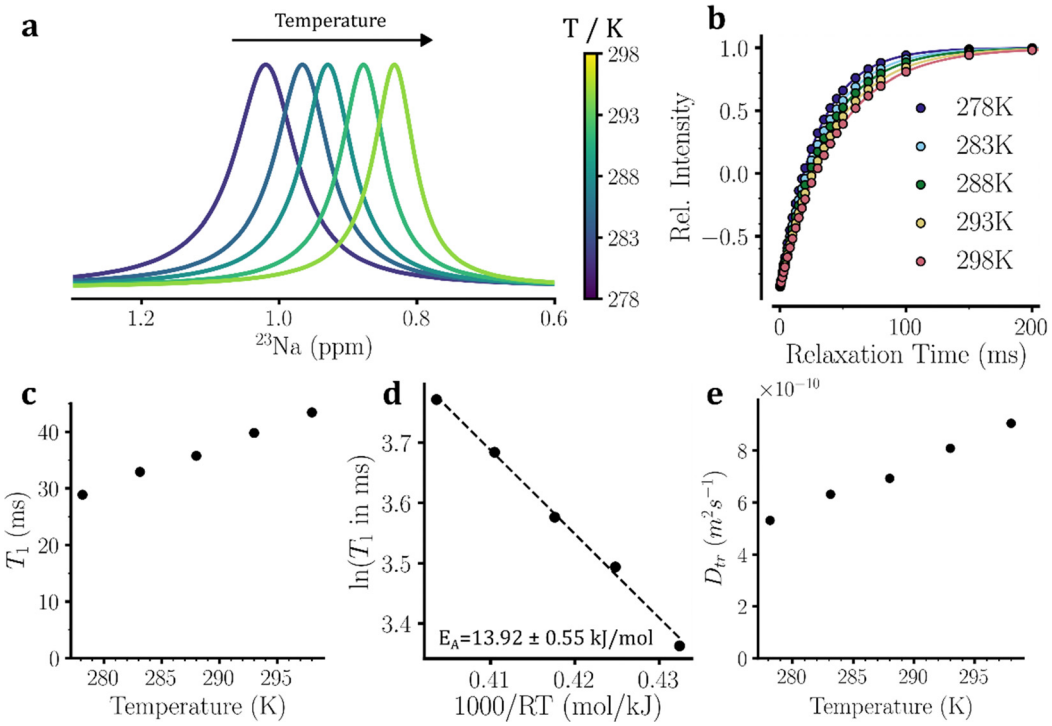

Fig. 4 ^{23}Na NMR-based probing of sodium ion mobility in eutectic NaCl solution. (a) 1D ^{23}Na NMR spectra of the eutectic NaCl solution at temperatures of 278–298 K. (b) ^{23}Na longitudinal spin–lattice (T_1) relaxation-based inversion-recovery data, shown for temperatures of 278–298 K. (c) ^{23}Na T_1 relaxation times as a function of temperature in the range 278–298 K. (d) Arrhenius analysis of the temperature dependence of ^{23}Na T_1 relaxation times. The slope of the fitted line represents (apparent) activation energy (E_A) for rotational mobility of sodium ions. (e) Diffusion coefficients of sodium ions measured through ^{23}Na-based pulse-field-gradient (PFG) NMR diffusion experiments, shown for temperatures of 278–298 K. The error bars shown in the different panels were derived from the standard error of the least-squares curve fitting and in some cases were smaller than the symbol size.

occurring in the fast extreme-narrowing regime. Likewise, the ^{35}Cl T_1 relaxation times increased from 16.308 ± 0.003 ms at 5 °C to 26.281 ± 0.004 ms at 25 °C. The corresponding T_2* relaxation times were 16.2 and 25.5 ms at 5 and 25 °C, which were again almost identical to the T_1 relaxation times in accordance with the fast extreme-narrowing dynamics of chloride ions. The (apparent) E_A determined through Arrhenius analysis of temperature dependence of ^{23}Na and ^{35}Cl T_1 relaxation times were 13.92 ± 0.55 and 16.14 ± 0.81 kJ mol^{-1}, respectively (Fig. 4(d) and 5(d)).

Diffusion of ions in eutectic NaCl solution

Next, we measured the diffusion coefficients of sodium and chloride ions in eutectic NaCl solution through ^{23}Na and ^{35}Cl-based PFG-NMR experiments (Fig. S10a and S11a, ESI†). The diffusion coefficients increased from 5.32 ± 0.02 × 10^{-10} m^2 s^{-1} and 8.30 ± 0.18 × 10^{-10} m^2 s^{-1} at 5 °C to 9.05 ± 0.02 × 10^{-10} m^2 s^{-1} and 12.92 ± 0.12 × 10^{-10} m^2 s^{-1} at 25 °C, respectively for sodium and chloride ions (Fig. 4(e) and 5(e)). The corresponding E_A obtained through Arrhenius analysis (Fig. S10b and S11b, ESI†) were 18.26 ± 0.79 and 15.22 ± 0.51 kJ mol^{-1}, respectively. In the case of ^{35}Cl ions, the diffusion and T_1 relaxation time-based E_A were within the experimental range of error identical, which, assuming a negligibly small contribution of the temperature dependence of EFG to ^{35}Cl T_1 relaxation times, is consistent with the high degree of coupling between the translational and rotational mobility of chloride ions. Notably, the E_A associated to chloride ion motions were significantly smaller than those of water molecules, suggesting that the motions of chloride ions and water molecules were (at least) partially independent from each other. On the other hand, the ^{23}Na ions exhibited a different behavior: their diffusion-based E_A was larger than the T_1 relaxation time-based E_A but close to that of water molecules. This is consistent with the scenario that the translational mobility of sodium ions and water molecules is coupled to a greater extent than that occurring between chloride ions and water molecules. Besides, if we assume a negligibly small contribution of the temperature dependence of EFG to ^{23}Na T_1 relaxation times, as we did for ^{35}Cl ions, the difference in diffusion and T_1 relaxation time-based E_A of ^{23}Na ions could then be interpreted as a significant degree of uncoupling between the translational and rotational mobility of sodium ions. This behavior is in contrast with what was observed for ^{35}Cl ions and may have its origin in the different ways of ion–water interactions between cations and anions.[21]

^{17}O T_1 relaxation of sulfate ions in eutectic $MgSO_4$ solution

Around 0.15% of sulfate ions (SO_4^{2-}) contain at least one ^{17}O nucleus, which as shown in Fig. S6, ESI,† exhibit a chemical shift well resolved from the ^{17}O nuclei of water molecules. The 1D ^{17}O NMR spectra of the eutectic $MgSO_4$ solution at

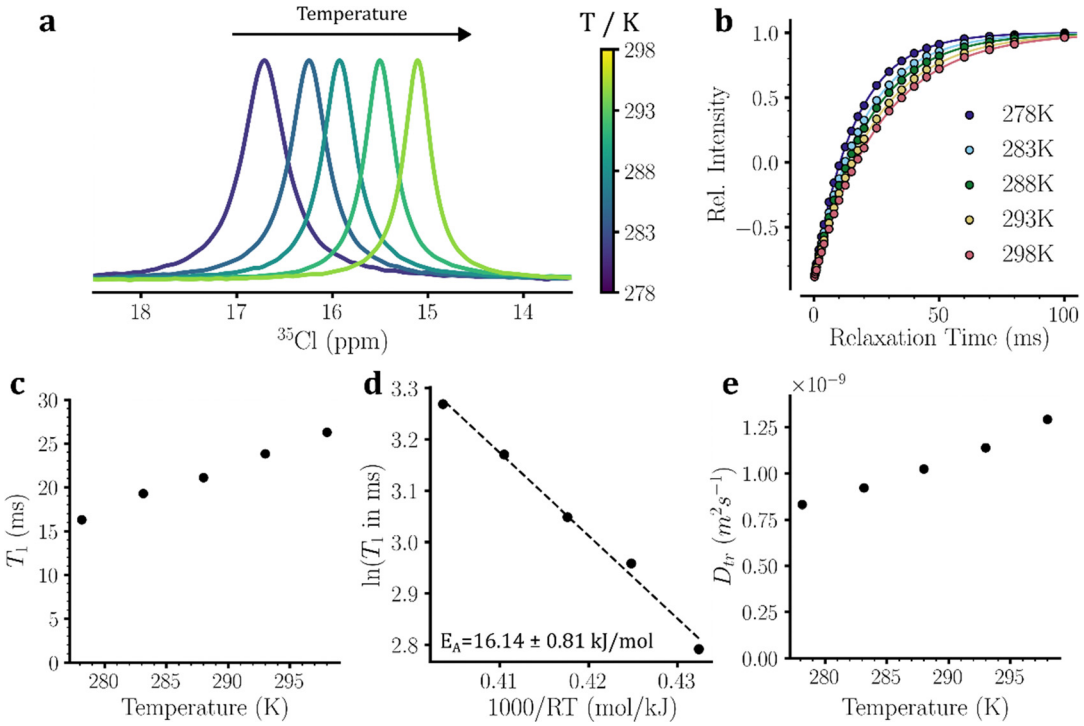

Fig. 5 ^{35}Cl NMR-based probing of sodium ion mobility in eutectic NaCl solution. (a) 1D ^{35}Cl NMR spectra of the eutectic NaCl solution at temperatures of 278–298 K. (b) ^{35}Cl longitudinal spin–lattice (T_1) relaxation-based inversion-recovery data, shown for temperatures of 278–298 K. (c) ^{35}Cl T_1 relaxation times as a function of temperature in the range of 278–298 K. (d) Arrhenius analysis of the temperature dependence of ^{35}Cl T_1 relaxation times. The slope of the fitted line represents (apparent) activation energy (E_A) for rotational mobility of sodium ions. (e) Diffusion coefficients of sodium ions measured through ^{35}Cl-based pulse-field-gradient (PFG) NMR diffusion experiments, shown for temperatures of 278–298 K. The error bars shown in the different panels were derived from the standard error of the least-squares curve fitting and in some cases were smaller than the symbol size.

temperatures 278–298 K are shown in Fig. 6(a). The inversion-recovery data demonstrated the temperature-dependent increase in the ^{17}O T_1 relaxation times of sulfate ions, in accordance with the faster rotational mobility of sulfate ions at higher temperatures (Fig. 6(b) and Fig. S12, ESI†). The ^{17}O T_1 relaxation times increased from 1.36 ± 0.19 ms at 278 K to 1.99 ± 0.18 ms at 298 K (Fig. 6(b)). The (apparent) E_A determined through Arrhenius analysis of temperature dependence of ^{17}O T_1 relaxation times was 13.25 ± 1.05 kJ mol^{-1} (Fig. 6(c)). Unlike ^{1}H and especially ^{17}O T_1 relaxation times of water (Fig. 1(d) and 2(d)), no clear change in slope was observed in the Arrhenius plot of ^{17}O T_1 of sulfate ions (Fig. 6(c)). In addition, the ^{17}O T_1-based estimated E_A of sulfate ions was significantly smaller than that of water molecules, suggesting that the rotational mobility of sulfate ions in the eutectic $MgSO_4$ solution is at least partially uncoupled from water molecules. Due to severe relaxation losses of ^{17}O NMR signals during diffusion delays, no diffusion measurement of sulfate ions was feasible.

Discussion

The ^{1}H and ^{17}O T_1 relaxation and ^{1}H NMR diffusion data (Fig. 1–3) show that water molecules have higher rotational and translational mobility in the eutectic NaCl than in the $MgSO_4$ solution across the temperature and pressure ranges potentially pertinent to the subsurface ocean of Europa. In the eutectic NaCl and $MgSO_4$ solutions, the ^{23}Na (Fig. 4) and ^{35}Cl (Fig. 5) relaxation and diffusion data of sodium and chloride ions and ^{17}O relaxation data of sulfate ions (Fig. 6) demonstrate various levels of coupling between rotational and translational mobility of these ions and surrounding water molecules (Table 1 and Fig. S13, ESI†).

The exact temperature of Europa's ocean is unknown, but various models predict a temperature between 0 and −4 °C.[6,36] While the $MgSO_4$ solution cannot go below −3.8 °C and remain a liquid, the temperature of Europa's ocean may be reduced by chlorine salt dissolution down to *ca.* −13 °C.[12,24] The lower temperatures are however very unlikely considering the chondritic origin of Europa and its compositional restriction in chlorine content.[12] Our NMR diffusion and relaxation data demonstrate that across the temperature range down to −13 °C (including the 0 to −4 °C range predicted for Europa's ocean), the translational (Fig. 3) and rotational mobility (Fig. 1) of water molecules are larger in the NaCl than in the $MgSO_4$ solution. The pressure dependence of water's proton relaxation time and diffusion was insignificant (or very small, in the case of ^{1}H T_1 of water in NaCl solution, Fig. 1(e)) across the pressure range of 1–500 bar corresponding to depth levels up to 38 km in Europa's ocean (Fig. 1(e) and 3(d)). It is therefore safe to suggest that the larger mobility of water molecules in the NaCl

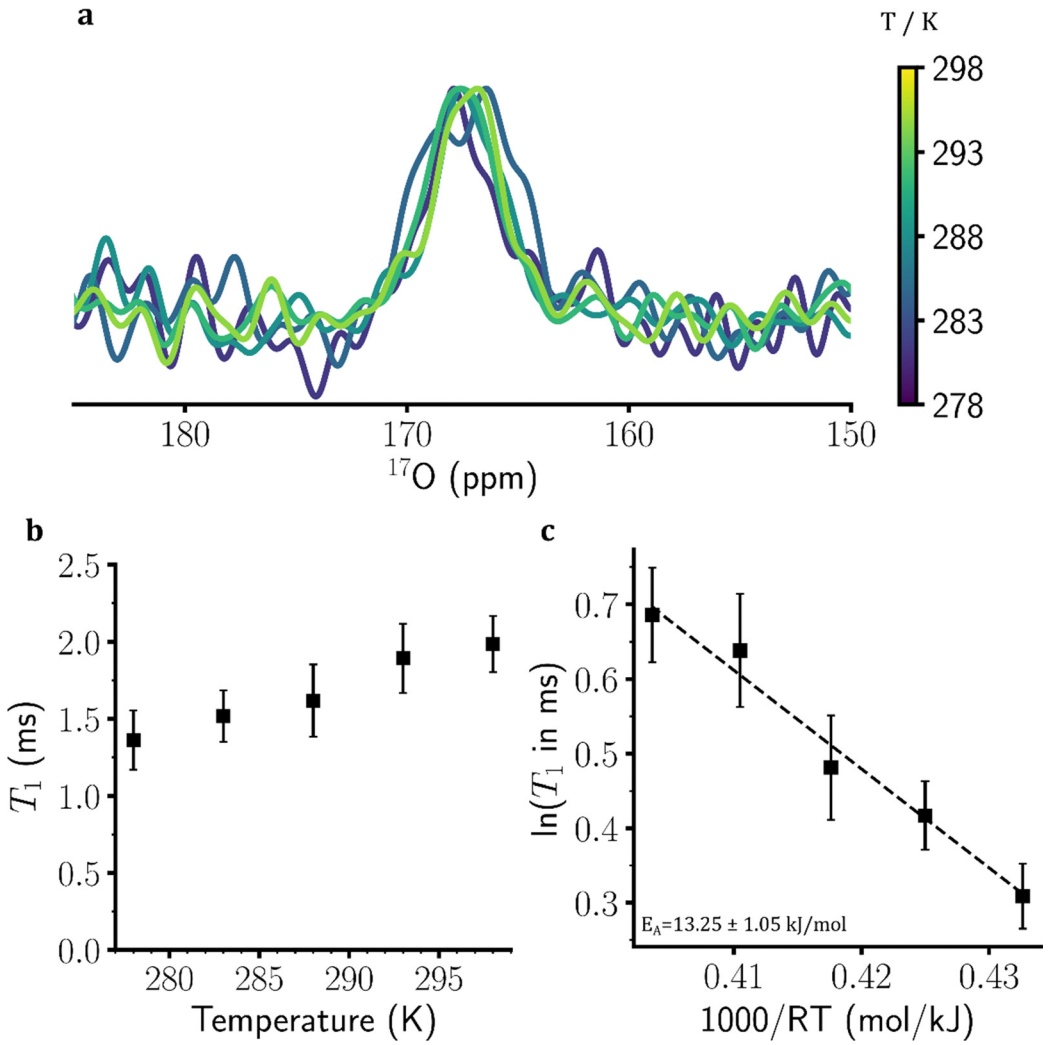

Fig. 6 ^{17}O NMR-based probing of sulfate ion's rotational mobility in eutectic $MgSO_4$ solution. (a) 1D ^{17}O NMR spectra of sulfate ions of the eutectic $MgSO_4$ solution measured at temperatures of 278–298 K. (b) ^{17}O T_1 relaxation times of sulfate ions as a function of temperature in the range of 278–298 K. (c) Arrhenius analysis of the temperature dependence of ^{17}O T_1 relaxation times of sulfate ions. The slope of the fitted line represents (apparent) activation energy (E_A) for the rotational mobility of sulfate ions.

compared with the $MgSO_4$ solution would remain the case up to pressures of 1300–2600 bar at the estimated 100–200 km depth levels of Europa's ocean.[2]

Biomolecules exert their activities through motions, which are closely coupled to water mobility.[19] There are habitats on Earth, *e.g.* hypersaline lakes, in which water activity, a quantity related to water mobility, becomes a limitation for organisms. Several halotolerant/halophilic archaea and prokaryotes are however capable of growing at such high salt concentrations,[37] even at saturated concentrations of NaCl or $MgSO_4$.[24] The estimated average salinity of Europa's ocean depends on the thickness of the icy shell of Europa (see *e.g.* ref. 6 for a recent estimation of salinity), but could reach the near-saturation concentrations in thin-shell models if the ice shell would be less than 15 km thick.[11] While the chondritic origin of Europa and its compositional restrictions make a globally near-saturated ocean a very unlikely scenario,[12] it is possible that the salinity reaches such high levels at the ocean–ice shell and ocean–seafloor boundaries. Recent simulations have shown that the pockets of salty liquid water (brines) existing in the ice shell of Europa can reach high salinity levels, which are still compatible with life.[38,39] Our NMR data show the higher mobility of water molecules in the highly concentrated eutectic NaCl compared with the $MgSO_4$ solution in temperatures pertinent to Europa's ocean and brine pockets near the ice shell–ocean interface. Considering the important role of water mobility in life-related processes, our data highlight the higher habitability potential of a NaCl-rich compared with a $MgSO_4$-rich Europa ocean.

Europa is regarded as one of the most promising candidates in the search for extraterrestrial life within the outer solar system.[2,24] The discovery of life on Europa would almost certainly imply a second origin of life independent from Earth and indicate that life could emerge relatively easily throughout the universe wherever its basic requirements are met. In addition to the presence of liquid water and a source of energy

required for maintaining the biomolecular system away from its thermodynamic equilibrium, a necessary condition for the emergence of life on Europa is the availability of a suite of elements such as H, C, N, O, P and S critical for building the most basic units of biomolecules. The ocean–seafloor and ocean–ice interface regions are expected to contain a higher concentration of these elements than the bulk ocean and support chemical reactions forming the most basic organic molecules. In the case of the ocean–ice boundary region, the nearby ice shell may harbor pockets of liquid water, in which the eutectic freezing could increase the concentration of simple organic and biomolecules even further and promote prebiotic chemistry such as polymerization reactions.[24] This process could further benefit from the exogenic delivery of organic materials by comets and meteorites onto the surface of Europa,[5] followed by their transport through subduction in the ice shell.[3] Furthermore, as has recently been shown,[38] a brine volume fraction higher than a certain critical porosity threshold could even establish a stable ''nutrient-open'' habitat near the ice–ocean interface, where transport of nutrients between the ocean and brine system would support a ''growth''-regime for viable microorganisms. Notably, at a pressure of 1 bar, the NaCl solution could support the presence of liquid water down to its eutectic temperature of *ca.* −22 °C in such water pockets, while the lowest liquid water-compatible temperature for $MgSO_4$ solution would be −4 °C. These eutectic temperatures are expected to be lowered at higher pressure levels of deep ice shells, however the difference between eutectic temperatures of NaCl and $MgSO_4$ solutions remains largely pressure-independent.[28] Our NMR data shows that water molecules retain a considerable level of translational and rotational mobility in the eutectic NaCl solution at around −22 °C, only slightly lower than water mobility in the eutectic $MgSO_4$ solution at *ca.* −4 °C. Recently, it has been suggested that the uniquely large and concentration-invariant mobility of water in potassium-containing salt solutions may play a role in the origination of life within the potassium-enriched confined environments on early Earth.[32] Considering the broader range of liquid water-compatible temperatures for NaCl, when compared to $MgSO_4$ solution, and the (relatively) large mobility of water molecules in NaCl solution even at temperatures as low as −22 °C, we suggest that NaCl has a higher potential than $MgSO_4$ to support the origination of life within the cold local environments of Europa's ice shell. Notably, a recent observation by the James Webb Space Telescope (JWST) demonstrated the presence of CO_2 concentrated in Tara Regio, likely to be originated from within Europa.[40] Our results could be relevant also for Enceladus, the small icy moon of Saturn, which has a subglacial ocean likely to contain NaCl as the dominant salt type.[41] In this regard, it is worth noting that various small and even large organic molecules have been detected in Enceladus plumes,[42–44] highlighting the potential of a NaCl-rich ocean to support prebiotic organic reactions.

A recent study demonstrates that water dynamics independent of dissolved ions play a crucial role in biomolecular self-assembly processes such as pathological protein aggregation.[45] In this regard, the NMR-based approach utilized in this study represents a powerful approach to quantify the mobility of water molecules and ions in biomolecular mixtures, thereby helping to disentangle the complex effect of ions on biological processes. Besides, the NMR-based quantification of water and ion dynamics can be used in various applications such as improving properties of hydrogels as drug delivery systems,[46] optimizing membranes used for water purification and desalination,[47] and developing optimal conditions for microfluidic devices.

Conclusions

Using ^1H and ^{17}O NMR diffusion and relaxation methods, we investigated the translational and rotational mobility of water molecules in NaCl and $MgSO_4$ solutions, the two salts that are likely to be ubiquitously present in Europa's subsurface ocean. The eutectic concentrations of these two salts were used in order to emulate the eutectic melts potentially existing within the ice shell of Europa and broaden the range of accessible temperatures down to their eutectic temperatures. Our data showed that water mobility in the eutectic NaCl solution is larger than in the eutectic $MgSO_4$ solution across a broad range of temperatures and pressures relevant for the Europa's subglacial ocean. Even at its much lower eutectic temperature of *ca.* −22 °C, the NaCl solution exhibited a water mobility only slightly lower than that of the $MgSO_4$ solution at its eutectic temperature of −3.8 °C. Considering the important role of water mobility in relation to the habitability and origination of life, our data point to the higher potential of an NaCl-rich Europa ocean to accommodate life and support the origination of life within the eutectic melts of the ice shell of Europa.

Author contributions

D. S.: investigation, formal analysis, visualization, writing – review & editing. N. R.-G.: conceptualization, methodology, investigation, formal analysis, validation, writing – original draft, writing – review & editing, supervision.

Conflicts of interest

There are no conflicts to declare.

Acknowledgements

N. R.-G. acknowledges the Deutsche Forschungsgemeinschaft (German Research Foundation, DFG) for research grant RE 3655/2-3. The generous access to NMR measurement time provided by Department of NMR-based Structural Biology, Max Planck Institute for Multidisciplinary Sciences is gratefully acknowledged.

Notes and references

1 N. W. Hinman, *Proced Earth Planet. Sci.*, 2013, 7, 354–359.

2 L. Carre, G. Zaccai, X. Delfosse, E. Girard and B. Franzetti, *Astrobiology*, 2022, **22**, 322–367.
3 S. A. Kattenhorn and L. M. Prockter, *Nat. Geosci.*, 2014, **7**, 762–767.
4 M. A. Pasek and R. Greenberg, *Astrobiology*, 2012, **12**, 151–159.
5 E. Pierazzo and C. F. Chyba, *Icarus*, 2002, **157**, 120–127.
6 Y. Ashkenazy and E. Tziperman, *Nat. Commun.*, 2021, **12**, 6376.
7 C. F. Chyba and K. P. Hand, *Science*, 2001, **292**, 2026–2027.
8 M. Y. Zolotov and E. L. Shock, *J. Geophys. Res. Planets*, 2001, **106**, 32815–32827.
9 M. Y. Zolotov and E. L. Shock, *J. Geophys. Res. Planets*, 2004, **109**, E06003.
10 M. M. Daswani, S. D. Vance, M. J. Mayne and C. R. Glein, *Geophys. Res. Lett.*, 2021, **48**, e2021GL094143.
11 K. P. Hand and C. F. Chyba, *Icarus*, 2007, **189**, 424–438.
12 J. S. Kargel, J. Z. Kaye, J. W. Head, G. M. Marion, R. Sassen, J. K. Crowley, O. Prieto Ballesteros, S. A. Grant and D. L. Hogenboom, *Icarus*, 2000, **148**, 226–265.
13 F. P. Fanale, Y. H. Li, E. De Carlo, C. Farley, S. K. Sharma, K. Horton and J. C. Granahan, *J. Geophys. Res. Planets*, 2001, **106**, 14595–14600.
14 W. B. McKinnon and M. E. Zolensky, *Astrobiology*, 2003, **3**, 879–897.
15 C. Schmidt and C. E. Manning, *Geochem. Perspect. Lett.*, 2017, **3**, 66–74.
16 S. K. Trumbo, M. E. Brown and K. P. Hand, *Sci. Adv.*, 2019, **5**, eaaw7123.
17 P. Valenti, R. J. Bodnar and C. Schmidt, *Geochim. Cosmochim. Acta*, 2012, **92**, 117–128.
18 K. Henzler-Wildman and D. Kern, *Nature*, 2007, **450**, 964–972.
19 J. R. Lewandowski, M. E. Halse, M. Blackledge and L. Emsley, *Science*, 2015, **348**, 578–581.
20 H. Ohtaki and T. Radnai, *Chem. Rev.*, 1993, **93**, 1157–1204.
21 H. J. Bakker, *Chem. Rev.*, 2008, **108**, 1456–1473.
22 Y. Marcus, *Chem. Rev.*, 2009, **109**, 1346–1370.
23 N. Kitadai and S. Maruyama, *Geosci. Front.*, 2018, **9**, 1117–1153.
24 K. P. Hand, C. F. Chyba, J. C. Priscu, R. W. Carlson and K. H. Nealson, in *Europa*, ed. R. T. Pappalardo, W. B. McKinnon and K. K. Kurana, University of Arizona Press, 2009, pp. 589–630, DOI: 10.2307/j.ctt1xp3wdw.32.
25 X. A. Mao, J. X. Guo and C. H. Ye, *Chem. Phys. Lett.*, 1994, **222**, 417–421.
26 X. A. Mao and C. H. Ye, *Concepts Magn. Reson.*, 1997, **9**, 173–187.
27 C. L. Van Dover, *The Ecology of Deep-Sea Hydrothermal Vents*, Princeton Univ., Princeton, New Jersey, 2000.
28 B. Chang, A. N. Consiglio, D. Lilley, R. Prasher, B. Rubinsky, B. Journaux and M. J. Powell-Palm, *Cell Rep. Phys. Sci.*, 2022, **3**, 100856.
29 I. P. Gerothanassis, *Prog. Nucl. Magn. Reson. Spectrosc.*, 2010, **56**, 95–197.
30 N. Rezaei-Ghaleh, F. Munari, S. Becker, M. Assfalg and C. Griesinger, *Chem. Commun.*, 2019, **55**, 12404–12407.
31 C. S. Johnson, *Prog. Nucl. Magn. Reson. Spectrosc.*, 1999, **34**, 203–256.
32 N. Rezaei-Ghaleh, *ChemistryOpen*, 2022, **11**, e202200080.
33 J. C. Fuentes-Monteverde, S. Becker and N. Rezaei-Ghaleh, *Protein Sci.*, 2021, **30**, 1315–1325.
34 S. C. Shekar, J. A. Tang and A. Jerschow, *Concepts Magn. Reson., Part A*, 2010, **36a**, 362–387.
35 P. S. Hubbard, *J. Chem. Phys.*, 1970, **53**, 985–987.
36 H. J. Melosh, A. G. Ekholm, A. P. Showman and R. D. Lorenz, *Icarus*, 2004, **168**, 498–502.
37 W. D. Grant, *Philos. Trans. R. Soc., B*, 2004, **359**, 1249–1266.
38 N. S. Wolfenbarger, M. G. Fox-Powell, J. J. Buffo, K. M. Soderlund and D. D. Blankenship, *Geophys. Res. Lett.*, 2022, **49**, e2022GL100586.
39 N. S. Wolfenbarger, M. G. Fox-Powell, J. J. Buffo, K. M. Soderlund and D. D. Blankenship, *J. Geophys. Res. Planets*, 2022, **127**, e2022JE007305.
40 G. L. Villanueva, H. B. Hammel, S. N. Milam, S. Faggi, V. Kofman, L. Roth, K. P. Hand, L. Paganini, J. Stansberry, J. Spencer, S. Protopapa, G. Strazzulla, G. Cruz-Mermy, C. R. Glein, R. Cartwright and G. Liuzzi, *Science*, 2023, **381**, 1305–1308.
41 M. Y. Zolotov, *Geophys. Res. Lett.*, 2007, **34**, L23203.
42 J. H. Waite, M. R. Combi, W. H. Ip, T. E. Cravens, R. L. McNutt, W. Kasprzak, R. Yelle, J. Luhmann, H. Niemann, D. Gell, B. Magee, G. Fletcher, J. Lunine and W. L. Tseng, *Science*, 2006, **311**, 1419–1422.
43 J. H. Waite, W. S. Lewis, B. A. Magee, J. I. Lunine, W. B. McKinnon, C. R. Glein, O. Mousis, D. T. Young, T. Brockwell, J. Westlake, M. J. Nguyen, B. D. Teolis, B. Niemann, R. L. McNutt, M. Perry and W. H. Ip, *Nature*, 2009, **460**, 487–490.
44 F. Postberg, N. Khawaja, B. Abel, G. Choblet, C. R. Glein, M. S. Gudipati, B. L. Henderson, H. W. Hsu, S. Kempf, F. Klenner, G. Moragas-Klostermeyer, B. Magee, L. Nolle, M. Perry, R. Reviol, J. Schmidt, R. Srama, F. Stolz, G. Tobie, M. Trieloff and J. H. Waite, *Nature*, 2018, **558**, 564–568.
45 A. D. Stephens, J. Kolbel, R. Moons, C. W. Chung, M. T. Ruggiero, N. Mahmoudi, T. A. Shmool, T. M. McCoy, D. Nietlispach, A. F. Routh, F. Sobott, J. A. Zeitler and G. S. Kaminski Schierle, *Angew. Chem., Int. Ed.*, 2023, **62**, e202212063.
46 M. J. Webber and E. T. Pashuck, *Adv. Drug Delivery Rev.*, 2021, **172**, 275–295.
47 R. Zhang, Y. Liu, M. He, Y. Su, X. Zhao, M. Elimelech and Z. Jiang, *Chem. Soc. Rev.*, 2016, **45**, 5888–5924.